High frequency asynchronous magnetic bead rotation for improved biosensors

Paivo Kinnunen,[1,2] Irene Sinn,[3] Brandon H. McNaughton,[1,2,3,a)] and Raoul Kopelman[1,2,3,b)]
[1]*Department of Chemistry, The University of Michigan, Ann Arbor, Michigan 48109, USA*
[2]*Department of Applied Physics, The University of Michigan, Ann Arbor, Michigan 48109, USA*
[3]*Department of Biomedical Engineering, The University of Michigan, Ann Arbor, Michigan 48109, USA*

(Received 16 April 2010; accepted 29 September 2010; published online 29 November 2010)

Biosensors with increasingly high sensitivity are crucial for probing small scale properties. The asynchronous magnetic bead rotation (AMBR) sensor is an emerging sensor platform, based on magnetically actuated rotation. Here the frequency dependence of the AMBR sensor's sensitivity is investigated. An asynchronous rotation frequency of 145 Hz is achieved. This increased frequency will allow for a calculated detection limit of as little as a 59 nm change in bead diameter, which is a dramatic improvement over previous AMBR sensors and further enables physical and biomedical applications. © *2010 American Institute of Physics*. [doi:10.1063/1.3505492]

Magnetic beads are used in a variety of applications, such as micro mixing,[1–3] analyte enrichment,[4–6] and biosensors.[7–11] Immunomagnetic separation and the availability of various magnetic bead biosensors allows for analyte isolation and detection with a single platform. Our current work concentrates on asynchronous magnetic bead rotation (AMBR) sensors, which have the capability of measuring changes in the sample over time, whereas much of the past work with magnetic bead biosensors has concentrated on analyte detection. AMBR has been previously utilized for sequential detection of individual bacterial cells in fluid.[7] Only recently have fluidic environments been incorporated into other high resolution sensing techniques, such as micromechanical oscillators,[12] allowing for real time studies of live cells.[13] Higher frequency AMBR allows more averaging, higher resolution and higher bandwidth studies, which will allow applications such as (1) real time single bacterium growth monitoring with subdiffraction limited sensitivity and (2) single virus detection, both in their given fluid environment.

In a rotating magnetic field, the motion of a ferromagnetic bead becomes asynchronous with the field above a critical driving frequency, Ω_c. The rotation in the synchronous regime (i.e., below the critical driving frequency) has been used for a variety of applications.[2,14] The AMBR approach concentrates on the asynchronous regime. The critical driving frequency for a ferromagnetic bead is a function of the permanent magnetic moment of the bead, m, the magnetic field strength, B, the shape factor, κ (which is 6 for a sphere), the kinematic viscosity, η, and the volume of the bead, V

$$\Omega_c = \frac{mB}{\kappa \eta V}. \tag{1}$$

Above the critical driving frequency, the (asynchronous) rotation frequency of the bead, $\langle \dot{\theta} \rangle$, is[15]

$$\langle \dot{\theta} \rangle = \Omega - \sqrt{\Omega^2 - \Omega_c^2}, \tag{2}$$

where Ω is the driving frequency. AMBR can also be performed with superparamagnetic beads; however, we limit our theoretical discussion here to ferromagnetic beads.

To date, the reported rotational frequencies for AMBR sensors have been between 0.2 and 29 Hz,[7,15–21] as summarized in Table I. Current AMBR applications, such as micromixing, pathogen detection, and growth studies could all benefit from higher rotational frequencies. We therefore investigate the AMBR probes' sensitivity, with respect to the bead rotation frequency, and demonstrate a system with a 49.15 Hz asynchronous rotation frequency, and achieve a 145 Hz critical frequency. The demonstrated system consists of a ferromagnetic bead driven with a 1 mT magnetic field in water. The experimental data is accurately described using ferromagnetic particle theory [Eq. (2)], with no observed contribution of superparamagnetic origin.[15,16]

Magnetic beads were prepared using a previously reported method.[22] A monolayer of 6.7 μm diameter polysty-

TABLE I. Reported critical frequencies of magnetically actuated asynchronously rotating systems in the literature. We designate $\langle \dot{\theta} \rangle_{max}$ as the approximate maximal rotational frequency of the driven system.

$\langle \dot{\theta} \rangle_{max}$ (Hz)	Driven system	Author
159	Elongated magnetic particles	Tierno[a]
145	Magnetic half coated beads	Current letter
29	Two bound magnetic particles	Ranzoni[b]
12	Magnetic microparticles	Janssen[c]
10	Magnetic carbon nanotubes	Korneva[d]
6.3	Magnetic hole systems	Helgesen[e]
2.4	Ferromagnetic beads	McNaughton[f]
1.08	Barium ferrite particles	McNaughton[g]
0.95	Magnetic microspheres	McNaughton[h]
0.2	Ferromagnetic beads	McNaughton[i]

[a]Reference 24.
[b]Reference 19.
[c]Reference 16.
[d]Reference 20.
[e]Reference 21.
[f]Reference 7.
[g]Reference 15.
[h]Reference 17.
[i]Reference 18.

[a)]Electronic mail: bmcnaugh@umich.edu.
[b)]Electronic mail: kopelman@umich.edu.

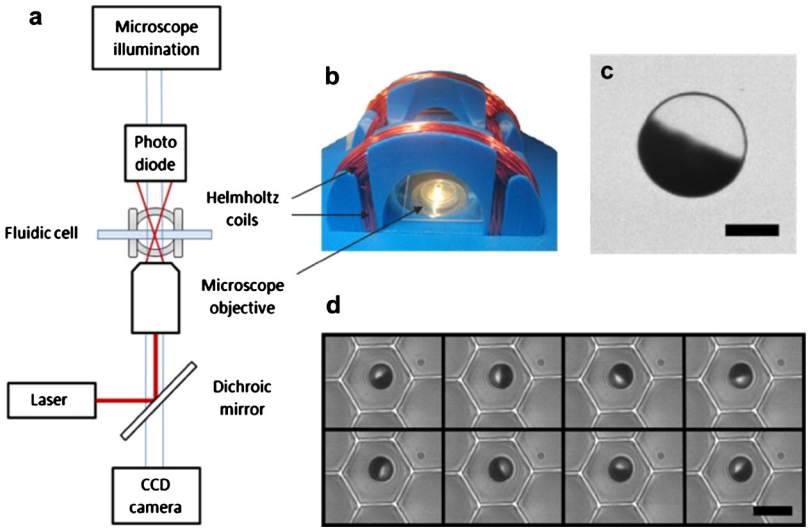

FIG. 1. (Color online) (a) Schematic representation of the laser and microscope setup in which a low power laser, in conjunction with a dichroic mirror, a microscope objective and a photodiode, was used to measure the rotation rate of a single magnetic bead. A digital camera can be used to simultaneously capture a video of the rotating system. (b) Custom designed Helmholtz coils were used to create a rotating magnetic field in the imaging plane. (c) An optical microscope image of a half coated 10 μm bead (300 nm Nickel coating) with a 5 μm scale bar. (d) Image sequence of a 6.7 μm bead rotating synchronously in the LiveCell Array in a 10 Hz field. The time between each frame is 14 ms and the scale bar is 10 μm.

rene particles (Spherotech TP-60–5) was coated with a 340 nm thick Nickel layer and magnetized in a 200 mT magnetic field, perpendicular to the surface. This process results in half-coated beads, where one side is nickel and the other hemisphere is polystyrene. The beads were resuspended in de-ionized and filtered water, with 0.5% of sodium dodecyl sulfate. Nunc, LiveCell Array slides (Thermo Fisher Scientific, Rochester) were used to keep each bead from significant translational movement during the experiment. The beads were placed in a rotating magnetic field where the rotation was analyzed; see Fig. 1 for a schematic of the system. A set of two custom built perpendicular Helmholtz coils was used to generate a rotating magnetic field with magnitudes of 0.25 to 1 mT, at frequencies 1 Hz to 1 kHz; Fig. 1(b).

The rotational frequencies of the magnetic beads, shown in Fig. 2, were measured by focusing a low power laser (633 nm, 2.5 mW) on the bead of interest and analyzing the modulation frequency of the deflected light; the light is modulated once during every bead rotation due to the nickel half coating. The light modulation could be measured by placing a 13 mm^2 photodetector above the sample, (Thorlabs, PDA36A) ~100 mm away and a few centimeters off-center of the laser beam exiting the sample. This was achieved by using a dichroic mirror that passes all wavelengths but that of the laser [Fig. 1(a)]. Measurements were taken on an inverted microscope (Olympus, IX 71) with a

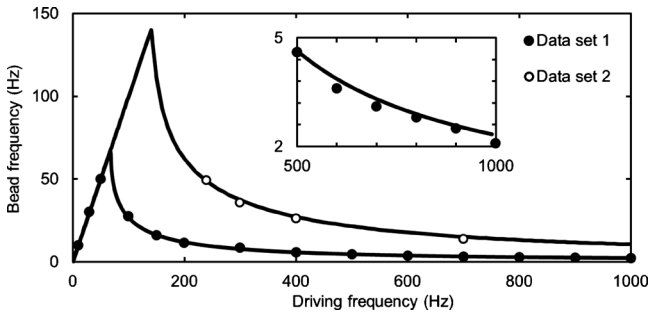

FIG. 2. The bead rotation frequency at varying driving frequencies for two 6.7 μm magnetic beads with rotating magnetic field strengths of 0.5 and 1 mT for data sets 1 and 2, respectively. The data is fitted with a single parameter least-squares method to the theory of a ferromagnetic bead in a rotating magnetic field [Eq. (1)]. Inset: Data set 1 zoomed in at the high driving frequency region, so as to demonstrate the quality of the fit.

photodetector, a data acquisition board (National Instruments, NI PCI-6221), and analyzed with a fast Fourier transform (FFT) routine, implemented in a LABVIEW (National Instruments) program. For Fig. 3, the rotation rates were determined using a digital camera (Basler, piA640–210gm); the videos were taken at 383 frames per second, and analyzed with IMAGEJ software by plotting a region of interest intensity over time and applying a FFT with a 512 point Dirichlet window (512 points equals 1.3 s).

In this letter, the sensitivity of the AMBR sensor, S, is defined as the smallest detectable change in the system's hydrodynamic radius, Δr, and it is governed by the uncertainty in the bead frequency measurement, $\Delta\langle\dot{\theta}\rangle$. The partial derivative method can be used to investigate how the uncertainty in the bead frequency $\Delta\langle\dot{\theta}\rangle$ affects the uncertainty in the bead radius

$$\Delta r = \left|\frac{\partial r}{\partial\langle\dot{\theta}\rangle}\right| \times \Delta\langle\dot{\theta}\rangle. \tag{3}$$

The radius r can be solved as a function of the bead frequency $\langle\dot{\theta}\rangle$, using Eqs. (1) and (2) and assuming a spherical bead. The partial derivative can be carried out and if a constant ratio $\langle\dot{\theta}\rangle/\Omega = 1/5$ is assumed (see Ref. 23), one obtains

$$\frac{\Delta r}{r} = \frac{1}{3} \times \frac{\Delta\langle\dot{\theta}\rangle}{\langle\dot{\theta}\rangle}. \tag{4}$$

Therefore, the relative uncertainty in bead radius is proportional to the relative measurement uncertainty and has no explicit frequency dependence. The sensitivity of the system is therefore

$$S = \frac{r}{3} \times \frac{\Delta\langle\dot{\theta}\rangle}{\langle\dot{\theta}\rangle}. \tag{5}$$

In order to measure the uncertainty of the bead rotation measurement, a 6.7 μm diameter magnetic bead AMBR sensor was driven with a 400 Hz, 1 mT rotating magnetic field and was continuously measured for 37 s. The data is shown in Fig. 3. The average rotation period was 25.4 Hz, with a 0.7 Hz standard deviation. Using these values and Eq. (5) to calculate the sensitivity, the AMBR sensor was found

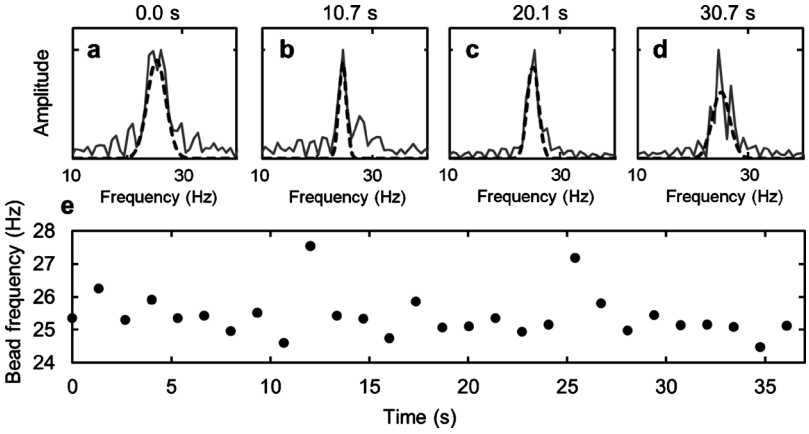

FIG. 3. The AMBR sensor signal in time. (a)–(d) FFT plots of rotation data, at time 0, 10.7, 20.1, and 30.7 s. (e) The rotational period of the AMBR sensor in time, as measured with the Fourier analysis, examples of which are shown in parts (a)–(d). The average of the bead frequency is 25.4 ± 0.7 Hz. The AMBR sensor is a 6.7 μm magnetic bead in 31 °C water.

to be sensitive to a 59 nm bead diameter change, which corresponds to a 4 femtoliters volume change. We anticipate that this sensitivity will allow for applications such as (1) real time single bacterium growth monitoring with subdiffraction limited sensitivity and (2) single virus detection, both in their given fluid environment.

To investigate the feasibility of the presented AMBR system for micro mixing applications, we calculated the maximum Reynolds number of the system[17] $\mathrm{Re}_{\max} \approx 1 \times 10^{-2}$. Although this value is low for micro mixing applications, it is be possible to achieve significantly higher Reynolds number values by increasing the magnetic field strength, bead size, amount of magnetic material, and/or by using a material with higher magnetic moment. For systems with a constant ratio of hydrodynamic volume to magnetic content volume, the critical rotational frequency remains constant for all sized particles. This suggests that Reynolds numbers of ~10 can be achieved with an order of magnitude larger bead having a nickel coating amounting to 5% of its diameter. Increased rotational frequencies of the magnetic beads reported in this letter were achieved by fabricating custom magnetic beads by thermally evaporating nickel onto nonmagnetic microparticles. Equation (2) was used to calculate the magnetic moment of the individual beads[17] with a 145 Hz critical frequency, 6.7 μm diameter, 1 mT magnetic field, 1 mPas dynamic viscosity, and a shape factor of 6 yielding $m \approx 8.6 \times 10^{-13}$ A m^2. Applications other than micromixing could be possible by the use of high frequency rotation, such as drag based binding affinity measurements. For example, the tension exerted onto a 10 nm long molecular tether attaching a 1 μm bead to the equator of a 6.7 μm ferromagnetic bead rotating synchronously at 145 Hz was estimated to be on the order of 1 pN; this value is large enough to break nonspecific bond interactions[8] (see Ref. 23).

In summary, we demonstrated high frequency AMBR measurements with up to 145 Hz critical driving frequency and calculated the resulting sensitivity of 59 nm change in the bead diameter, corresponding to a 4 femtoliters volume change. This sensitivity could allow for improved single bacterium growth monitoring and single virus detection. Furthermore, the high frequency rotation regime might also be used for applications such as micromixing and binding affinity measurements.

The authors thank Alex Hrin for creating a LabVIEW program for video capture. Support for this research was provided by NSF Grant No. DMR0455330 (R.K.) and NIH Grant No. R21EB009550 (R.K.). BHM was partially supported by NIH Grant No. UL1RR024986 (Postdoctoral Translational Scholar Program). The facilitites used for this research include the Michigan Nanofabrication Facility (MNF) at the University of Michigan. BHM discloses financial interest in Life Magnetics, Inc.

[1] A. Vuppu, A. Garcia, and M. Hayes, Langmuir **19**, 8646 (2003).
[2] S. L. Biswal and A. P. Gast, Anal. Chem. **76**, 6448 (2004).
[3] A. Rida and M. A. M. Gijs, Anal. Chem. **76**, 6239 (2004).
[4] S. Miltenyi, W. Müller, W. Weichel, and A. Radbruch, Cytometry **11**, 231 (1990).
[5] O. Olsvik, T. Popovic, E. Skjerve, K. S. Cudjoe, E. Hornes, J. Ugelstad, and M. Uhlen, Clin. Microbiol. Rev. **7**, 43 (1994).
[6] P. A. Chapman and C. A. Siddons, J. Med. Microbiol. **44**, 267 (1996).
[7] B. H. McNaughton, R. R. Agayan, R. Clarke, R. G. Smith, and R. Kopelman, Appl. Phys. Lett. **91**, 224105 (2007).
[8] D. R. Baselt, G. U. Lee, M. Natesan, S. W. Metzger, P. E. Sheehan, and R. J. Colton, Biosens. Bioelectron. **13**, 731 (1998).
[9] Y. R. Chemla, H. L. Grossman, Y. Poon, R. McDermott, R. Stevens, M. D. Alper, and J. Clarke, Proc. Natl. Acad. Sci. U.S.A. **97**, 14268 (2000).
[10] J. Connolly and T. G. St Pierre, J. Magn. Magn. Mater. **225**, 156 (2001).
[11] Q. A. Pankhurst, J. Connolly, S. K. Jones, and J. Dobson, J. Phys. D: Appl. Phys. **36**, R167 (2003).
[12] B. Ilic, D. Czaplewski, M. Zalalutdinov, H. G. Craighead, P. Neuzil, C. Campagnolo, and C. Batt, *The 45th International Conference on Electron, Ion, and Photon Beam Technology and Nanofabrication* (AVS, Washington, DC, 2001), pp. 2825–2828.
[13] M. Godin, F. F. Delgado, S. Son, W. H. Grover, A. K. Bryan, A. Tzur, P. Jorgensen, K. Payer, A. D. Grossman, M. W. Kirschner, and S. R. Manalis, Nat. Methods **7**, 387 (2010).
[14] T. Roy, A. Sinha, S. Chakraborty, R. Ganguly, and I. K. Puri, Phys. Fluids **21**, 027101 (2009).
[15] B. H. McNaughton, K. A. Kehbein, J. N. Anker, and R. Kopelman, J. Phys. Chem. B **110**, 18958 (2006).
[16] X. J. A. Janssen, A. J. Schellekens, K. van Ommering, L. J. van Ijzendoorn, and M. W. J. Prins, Biosens. Bioelectron. **24**, 1937 (2009).
[17] B. H. McNaughton, R. R. Agayan, J. X. Wang, and R. Kopelman, Sens. Actuators B **121**, 330 (2007).
[18] B. H. McNaughton, P. Kinnunen, R. G. Smith, S. N. Pei, R. Torres-Isea, R. Kopelman, and R. Clarke, J. Magn. Magn. Mater. **321**, 1648 (2009).
[19] A. Ranzoni, X. J. A. Janssen, M. Ovsyanko, L. J. van IJzendoorn, and M. W. J. Prins, Lab Chip **10**, 179 (2010).
[20] G. Korneva, H. Ye, Y. Gogotsi, D. Halverson, G. Friedman, J. C. Bradley, and K. G. Kornev, Nano Lett. **5**, 879 (2005).
[21] G. Helgesen, P. Pieranski, and A. T. Skjeltorp, Phys. Rev. A **42**, 7271 (1990).
[22] B. H. McNaughton, V. A. Stoica, J. N. Anker, K. M. Tyner, R. Clarke, and R. Kopelman, "Fabrication of Nanoparticles and Microspheres with Uniform Magnetic Half-Shells," Materials Research Symposia Proceedings, No. 988 (Materials Research Society, Warrendale, PA, 2006), p. 899E.
[23] See supplementary material at http://dx.doi.org/10.1063/1.3505492 for further discussion.
[24] P. Tierno, J. Claret, F. Saqués, and A. Cēbers, Phys. Rev. E **79**, 021501, (2009).